

PAPER • OPEN ACCESS

Recent on-beam tests of wide angle neutron polarization analysis with a ^3He spin filter: Magic PASTIS on V20 at HZB

To cite this article: E Babcock *et al* 2017 *J. Phys.: Conf. Ser.* **862** 012002

View the [article online](#) for updates and enhancements.

You may also like

- [The quest for solvable multistate Landau-Zener models](#)
Nikolai A Sinitsyn and Vladimir Y Chernyak
- [Discussion on data correction for Polarization Analysis with a \$^3\text{He}\$ spin filter analyzer](#)
Earl Babcock, Zahir Salhi, Emmanuel Kentzinger et al.
- [Simulation and optimization of a new focusing polarizing bender for the diffuse neutrons scattering spectrometer DNS at MLZ](#)
K Nemkovski, A Ioffe, Y Su et al.

PRIME
PACIFIC RIM MEETING
ON ELECTROCHEMICAL
AND SOLID STATE SCIENCE

HONOLULU, HI
Oct 6-11, 2024

Abstract submission deadline:
April 12, 2024

Learn more and submit!

Joint Meeting of
The Electrochemical Society
•
The Electrochemical Society of Japan
•
Korea Electrochemical Society

Recent on-beam tests of wide angle neutron polarization analysis with a ^3He spin filter: Magic PASTIS on V20 at HZB

E Babcock^{1*}, Z Salhi¹, R Gainov^{2,3}, R Woracek⁴, H Soltner³,
P Pistel³, F Beule⁵, K Bussmann⁶, A Heynen³, H Kämmerling³,
F Suxdorf⁵, M Strobl⁴, M Russina², J Voigt⁶, A Ioffe¹

¹Jülich Centre for Neutron Science (JCNS) at Heinz Maier-Leibnitz Zentrum (MLZ),
Forschungszentrum Jülich GmbH, 85747 Garching, Germany

²Helmholtz-Zentrum Berlin für Materialien und Energie GmbH (HZB), Hahn-Meitner-Platz 1,
14109 Berlin, Germany

³Zentralinstitut für Engineering und Technologie (ZEA-1), Forschungszentrum Jülich GmbH,
52425 Jülich, Germany

⁴European Spallation Source ERIC, S-221 00 Lund, Sweden

⁵Jülich Centre for Neutron Science (JCNS) and Institute for Complex Systems (ICS)
Forschungszentrum Jülich GmbH 52425 Jülich, Germany

⁶Jülich Centre for Neutron Science (JCNS) and Peter Grünberg Institut (PGI), JARA-FIT
Forschungszentrum Jülich GmbH, 52425 Jülich, Germany

E-mail: e.babcock@fz-juelich.de

Abstract. A complete XYZ polarization analysis solution is under development for the new thermal time of flight spectrometer TOPAS [1], to be operated in the coming east neutron guide hall at the MLZ. Polarization Analysis Studies on a Thermal Inelastic Spectrometer, commonly called PASTIS [2], is based on polarized ^3He neutron spin filters and an XYZ field configuration for the sample environment and a polarization-preserving neutron guide field. The complete system was designed to provide adiabatic transport of the neutron polarization to the sample position while maintaining the homogeneity of the XYZ field. This system has now been tested on the polarized time-of-flight ESS test beam line V20 at HZB [3]. Down to the minimum wavelength of 1.6 Å on the instrument, the magnetic configuration worked ideally for neutron spin transport while giving full experimental freedom to change between the X, Y or Z field configuration. The ^3He cell used was polarized at the ^3He lab of the JCNS at the MLZ in Garching and transported to HZB in Berlin via car showing that such a transport is indeed feasible for such experiments. We present results of this test and the next steps forward.

1. Introduction

Beginning with the advent of ^3He polarization of practical magnitudes for neutron polarization and analysis, there have been proposed uses in wide-angle polarization analysis, especially for neutron spectrometry using high energy neutrons [4]. This idea developed into a uniform magnetic field insert housing a large-angle ^3He cell that can be placed around the sample environment of a typical wide-angle neutron spectrometer allowing polarization analysis over the full detector angle using a moderately sized ^3He cell and having minimal instrument modifications. One such application has been shown at NIST on the MACS spectrometer,



however here only for “Z” polarization analysis, i.e. for the magnetic field perpendicular to the scattering vector. [5]. The full polarization analysis version of such a system has become known in the community by its acronym PASTIS, for Polarization Analysis on a Thermal Inelastic Spectrometer [2]. Several projects towards such systems are in development at the ILL [6, 7], ISIS [8], SNS [9] plus our upcoming spectrometer projects at the ESS, TREX and DREAM [10] as well as the system described here for use on TOPAS [1] and NEAT at HZB in the meantime [11].

The motivation for use of a ^3He spin filter in these is again largely due to the polarized ^3He “idealized” characteristics as a neutron analyzer which would not have alignment or sample size dependencies while having a deterministic neutron energy/wavelength dependence which can then be used on neutrons of arbitrarily high energy and high inelastic neutron energy transfer. Other neutron polarization analysis methods such as wide-angle neutron super mirrors have been applied for wide-angle diffraction and spectroscopy, but normally for cold-spectrum neutron instruments (i.e. approximately wavelengths greater than 2.4 \AA or less than 15 meV energy) due to the limitations of the high-energy neutron reflectivities of such devices [9, 12, 13]. For a thermal neutron spectrometer such as TOPAS [1] which will use incident neutron energies of up to 165 meV or 0.7 \AA such devices would not provide the required performance leading us to work to further develop the magic PASTIS concept taking advantage of the characteristics of ^3He spin filter cells like the other groups cited earlier [5, 8, 9, 10].

This proceeding will summarize recent on-beam testing of the JCNS Magic PASTIS system in experiments on the V20 ESS test beamline at Helmholtz Zentrum Berlin.

2. Magic PASTIS, from concept to prototype

Magic PASTIS was not only designed to yield a good ^3He lifetime or T_1 performance, but also to ensure fully adiabatic transport of the neutron polarization to the sample position. The PASTIS system plus neutron guide fields have been reported previously [1, 14]. In some ways this concept bears resemblance to the PASTIS 2.0 implemented at the Institut Laue Langevin [7], however the details of the magnetic systems are different, and while our system has small dead angles of around 3 degrees every 90 degrees in the horizontal plane, the vertical opening is higher than the ILL PASTIS 2.0, on the order of 40 degrees, and matched to the out-of plane vertical acceptance of our TOPAS detector systems. In laboratory measurements a large 22 cm outside diameter doughnut-shaped cell named “Homer” was used to experimentally optimize the field gradients. The cell which is filled to 0.5 bar ^3He pressure gave a ^3He lifetime in excess of 50 hours in each of the three field directions was reported in [14]. This value of T_1 obtained with a ^3He cell translates to a maximum magnetic field gradient of less than $1 \times 10^{-3} \text{ cm}^{-1}$ over the volume of the cell, and a magnetic plus dipole-dipole limited ^3He lifetime in excess of 100 hours for cells of over 1 bar pressure [14].

Similarly, the guide field system was constructed and commissioned first in laboratory conditions. The description of this guide field system was reported in [1] and it has recently been assembled. The results of the bench test in Jülich using a hall probe met the expectations from the calculations and also permitted us to test the newly developed control software for automation of the PASTIS power supplies. Finally a polarized ^3He cell was transported from Garching. The results of this test were twofold, 1: we verified that we can polarize a cell in Garching and transport it by car over large distances, 2: we did not observe adverse effects on the ^3He lifetime due to the addition of the guide fields via a measurement of the cell lifetime in Jülich using NMR free-induction decay measurements of the ^3He polarization over time. Directly after the positive verification of this test, the magic PASTIS coil system and guide fields plus power supplies and control electronics were shipped via courier transport to HZB in Berlin for the neutron tests on V20.

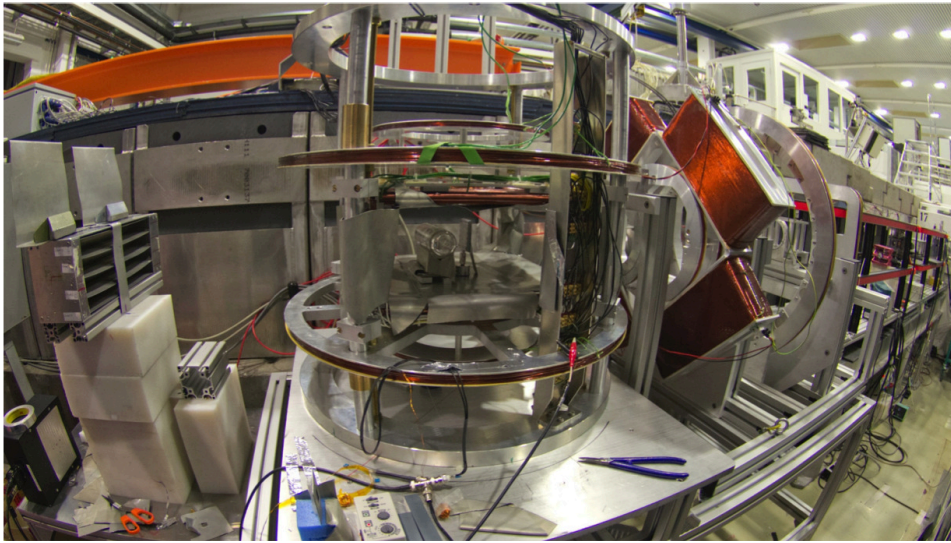


Figure 1. Photo of the magic PASTIS system and neutron X-Y-Z guide fields on V20. Right to left, the X-Y-Z guide fields and the incoming beam flight path, a sample in an aluminum cell in the center of PASTIS, the $D=4.3$ cm by $L=15$ cm ^3He cell used for analysis, and the four 40 cm neutron detectors mounted horizontally.

3. Magic PASTIS installed on V20

Using the experimental setup of V20 we have conducted the test of magic PASTIS in realistic conditions. The particular goals were to utilize the interface and test the practical handling of the system while obtaining the performance with polarized incident neutrons. Earlier tests of PASTIS systems, such as the tests on IN3 [2] showed that care must be taken with the guide fields to insure neutron polarization transport. Therefore this test was important to fully ensure and experimentally verify the neutron polarization transport beyond the expectations from calculations or field mapping.

The V20 instrument is a “test” beam line and is therefore very adaptable and has a very open geometry for installation of equipment [3]. The instrument essentially consists of a chopper system which can replicate the European Spallation Source (ESS) -proposed pulse structure [10, 15], an incident beam super-mirror bender polarizer, and a 6 m (can be extended to more than 10 m) open neutron flight path with adaptable detector options. The instrument’s bender polarizer provided a good polarization over the range of our measurement. From data taken during this experiment with two different ^3He cells of the polarized and unpolarized neutron transmissions we determined the incident beam polarisation efficiency P_p to be above 97.5% for neutron wavelengths from 1.6 Å to 6.5 Å (see figs. 3,5).

Using a polarized ^3He cell, we also optimised an RF gradient (neutron AFP) flipper by simply maximizing the obtained neutron flipping ratio, i.e. the ratio of the flipper-off transmission to the flipper-on transmission as a function of neutron wavelength (see fig. 3). A photo of the RF-gradient flipper is shown in fig. 2. The gradient field was created with a stack of 4 strong 50 mm x 12 mm x 25 mm NbFeB magnets on either side of the double 1 mm thick iron pole plates top and bottom with 10 mm thick iron pillars on the other side to close the magnetic flux return path. This gives a smooth gradient field that varied from about 50 G on the incident side to 10 G on the exit of the 35 cm length. The RF field was created with a “Gachinga” style resonator coupled to a double-parallel 40 turn coil which had higher turn density in the middle of the 30 cm long coil. The resonator is simply a high current transistor driven LRC

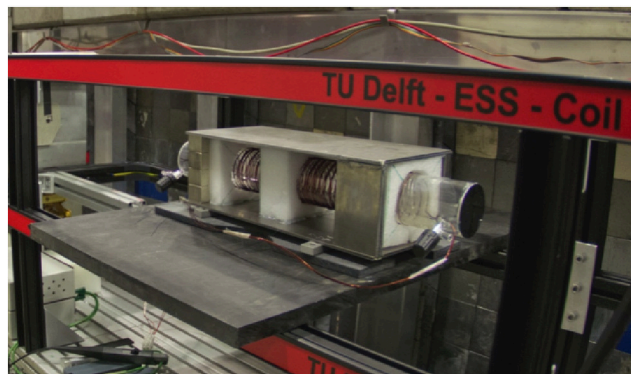


Figure 2. Photo of the neutron RF gradient flipper. The RF coil in the middle is wound on a glass tube with silicon windows that can be filled with ^4He when desired. The NbFeB magnet stacks are to the left, and the thick iron pillars to the left. The arrangement produces a relatively smooth gradient field that varies from 50 G on the NbFeB magnet side to 10 G on the other.

oscillator that uses the coil for L and one tunes to the desired resonance by adjusting C. The coil and gradient field of this flipper was placed inside of the race-track style coils which are used to create a nominal 10 G neutron guide field over the instrument flight path for neutron polarization preservation. Operating the RF at a frequency of 88 kHz we obtained the maximum flipping ratios for 2.5 amps current. The resulting total neutron polarization was described by a $P_n = P_p \tanh(P_{He} \Theta \lambda)$ dependence very well where the flipping ratio $F(\lambda)$ is related to the beam polarization $P_n(\lambda)$ by $F(\lambda) = (1 + P_n(\lambda))/(1 - P_n(\lambda))$. Here P_p is incident beam polarization, λ the neutron wavelength, Θ the ^3He cells pressure-length-cross section product and P_{He} the cells ^3He polarization. Data for F in the three orthogonal directions is shown in fig. 3.

The ^3He polarization and density-length product can be determined independently from neutron polarization by measuring the unpolarized neutron transmission over neutron wavelength for the polarized and un-polarized ^3He cell in time of flight as described in [16]. Taking the ratio of polarized (T_p) to unpolarized (T_0) transmission gives $T_p(\lambda)/T_0(\lambda) = \cosh(P_{He} \Theta \lambda)$ which can be fit to determine P_{He} and Θ , such data is shown in sec. 4 fig. 5. The same measurement performed for the “Mary” cell used in the flipper optimization measurements gave us a value of ^3He polarization of 39% at the time of the end of the measurement and a pressure-length product of 17.5 bar cm.

These measurements also helped us verify the adiabaticity of the neutron guide fields in the 3 orthogonal directions of PASTIS as each direction gave equivalent flipping ratios. Given the deterministic nature of the neutron polarization from polarized ^3He over wavelength, any deviation from the $P_p \tanh(P_{He} \Theta \lambda)$ dependence would imply a non-uniform incident beam polarization resulting from the incident beam polarizer, non-ideal flipping efficiency or polarization losses in the neutron transport. The latter case is ruled out because all three of the orthogonal directions of the PASTIS system and guide fields gave the same smooth $P_p \tanh(P_{He} \Theta \lambda)$ dependence and if there were a weak beam depolarization, it would neither be uniform over neutron wavelength nor is it likely that it would remain the same for the three very different field configurations of the PASTIS system. Also the flipper efficiency is assumed high as it is an adiabatic device and any deviation from adiabaticity would exhibit itself as oscillations in neutron polarization over neutron wavelength below a maximum value limited by the product of the incident beam polarization and ^3He analyzing power, especially at low wavelength. Incidentally, a slightly non-adiabatic neutron guide field would exhibit itself in the same way. Because we do not see such oscillations, and since this measurement gives us a

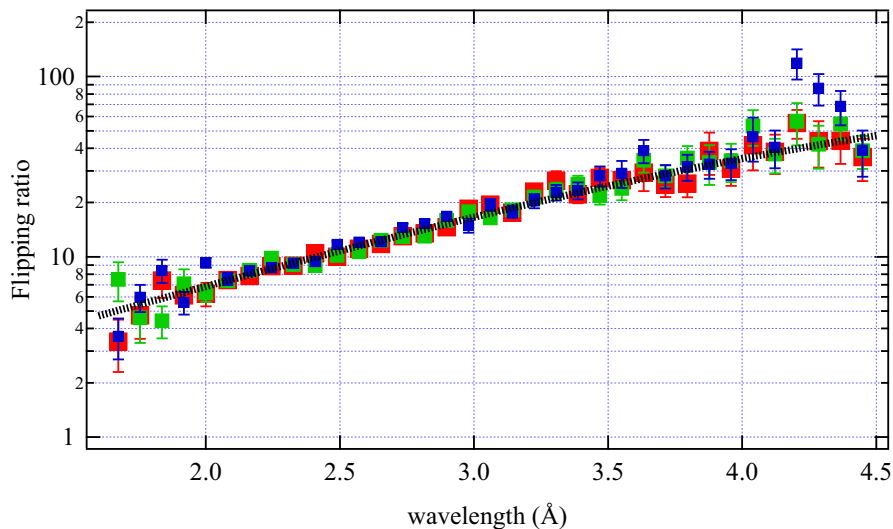


Figure 3. (Total neutron flipping ratio F_n which is related to the total neutron polarization P_n) by $F = (1 + P_n)/(1 - P_n)$ for each of the three orthogonal field orientations after optimization of the RF gradient flipper using the “Mary” cell which had 17.5 bar cm of ^3He and a polarization of 39% at the time of this measurement. Red is the vertical direction “Y”, blue is the transverse direction “X” and green in the longitudinal direction “Z”. This cell had a higher opacity (product of ^3He pressure and length) than the cell used for the overnight measurements, thus it had very low transmission above 4.5 Å for the dark state, i.e. incident beam polarization antiparallel to the ^3He analyzer polarization so the flipping ratios above this wavelength are noise/background limited. The dotted black line is a fit assuming a $P_n = P_p \tanh(P_{He}\Theta\lambda)$ dependence of the neutron polarization. This data allows us to conclude the incident beam polarization can be considered uniform with adiabatic transport in the X, Y and Z field directions over the range of neutron wavelengths we used .

P_p consistent with the overnight measurements in sec. 4 and gives P_{He} values consistent with the independent measurements of P_{He} from unpolarized neutron transmission, we conclude the polarization transport to be adiabatic and the flipper efficiency to be high within the errors of the measurement.

After the race-track guide fields, we placed our TOPAS X-Y-Z guide fields and the PASTIS system, as one can see in the photo of fig. 1. The guide fields plus PASTIS require a total of 11 independently set power supplies, and a 90° rotation of one of the permanent-magnet Halbach rings to obtain the 3 orthogonal field configurations. For this test the Halbach ring rotation was not automated, but simply rotated by hand between the two configurations required. The large number of power supplies did however require automation, to prevent errors as well as to minimise the time required to switch between field directions and thus minimize possible losses in ^3He polarization due to higher field gradients while switching. For this purpose we set the Delta-Elektronika power supplies via a profi-bus interface that was addressed over an ethernet port by a control computer running a PYTHON application and GUI. A screen shot of the GUI is shown in figure 4. This interface allowed us to set the default currents for all of the power supplies and enable and disable them in groups corresponding to the 3 orthogonal field directions. The application also insured that there is always one field ON in the PASTIS system, and enables the new set direction for the holding field before shutting off the prior field with a small time delay. After configuring the currents to the previously determined optimal values in

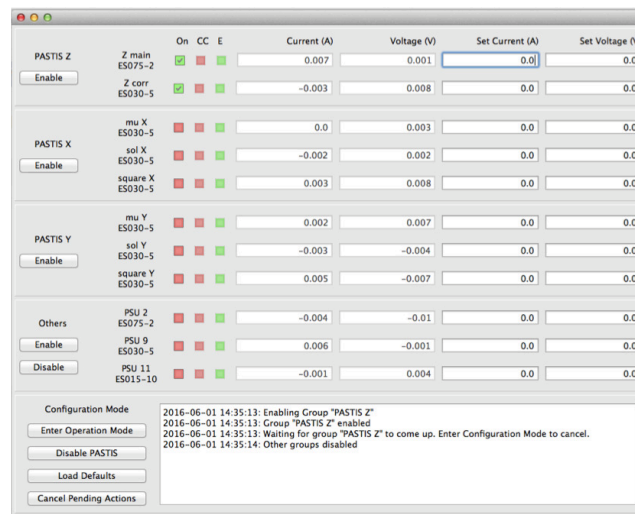


Figure 4. Screen shot from the GUI interface for control of PASTIS and the PASTIS guide field systems. This simple interface allows us to easily set the currents on the PASTIS power supplies and lock them to the given value. Once the current defaults for all the power supplies are set, this GUI allows one to simply “choose” the field direction with the press of a virtual button, which can be performed directly in this GUI or via a tcip command. The program prevents the inadvertent depolarisation of the ^3He cells during field switching by locking the set currents, and ensuring that the ^3He cell is always in an appropriate magnetic field during operation mode.

the GUI, one enters the operation mode and can simply give a command (mouse click) to choose the X, Y or Z field direction. This command can also be sent from any eventual instrument control computer and be integrated into measurement scripts.

4. Over-night measurement of cell parameters

After optimization of the installation and neutron flipper a “fresh” ^3He cell was transported from Garching and installed for measurements. A suitable c-shaped cell was not available for this measurement so we used a $D=4.3$ cm by $L=15$ cm cylindrical cell which has a 230 hour ^3He T_1 in laboratory conditions and 3.29 bar of ^3He . The cell cylindrical axis was placed perpendicular to the neutron beam off-center in the PASTIS coils behind a sample holder in the middle (see fig. 1). This cell is of comparable size and pressure to an eventual c-shaped cell optimized for a cold neutron spectrum, which would provide a neutron polarization of 94% at 2.4 Å with an initial ^3He polarization of 70% for example. This cell’s 14.2 bar cm neutron path length in this configuration clearly doesn’t compare to the approximately 30+ bar cm that will be required for the thermal neutron spectrum of TOPAS, production of suitable high performance cells for both the cold-neutron spectrum on NEAT and the thermal-neutron spectrum of TOPAS is the topic of continuing work [17].

The cell was removed from the polarizer at the MLZ in Garching at around 9 am and was eventually installed in PASTIS on V20 at around 7 pm. Using measurements of the flipping ratio and total transmission over time we were able to characterize the ^3He polarization of the cell. For each flipping ratio measurement, the PASTIS system was set to a different direction. Performing a global analysis of the transmission data taken from 7:30 pm until approximately noon the next day, shown in figure 5, we were able to determine the initial ^3He polarization of 50 % and on-beam lifetime of 109 hours. During this overnight measurement, the field direction was switched a total of 10 times, with measurements of the transmitted and the scatted beam

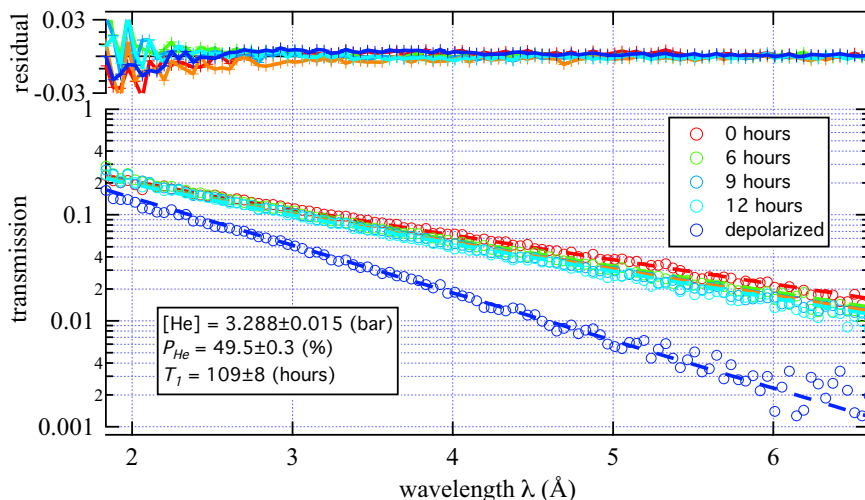


Figure 5. (Neutron transmission) Graph of the neutron transmission vs wavelength at different times and field orientations during our overnight measurement. A global analysis of this data gives a ${}^3\text{He}$ $T_1 = 109$ hours and an initial polarization of $P_{\text{He}} = 49.5\%$.

from a sample for the two neutron polarizations (flipper On and flipper Off) acquired for each field setting. The transmission measurements were typically recorded for 5 min each, and 1 hour each for the scattered beam. The starting polarization of 49.5 % is certainly not optimal but was sufficient for this test. Considering the transport via car and the 10 hour delay after polarization this value was a positive first result that we believe can be improved upon with further experience. The eventual regular use of this device on TOPAS will be in Garching where the cell polarization will take place nearby the instrument further helping to minimize any polarization losses during cell transportation. For the data acquisition, the position-sensitive-detector was not yet available on V20, thus we used an array of 4, 40 cm long ${}^3\text{He}$ detector tubes placed horizontal in order to achieve a wide effective Q-range. A beam stop was made of cadmium and was attached to the detector housing such that the transmitted beam could be blocked for the scattering measurements, and conversely extra cadmium masks were also attached to the detectors to block the scattered neutron beam while performing transmission measurements.

The sample used was a hydrated graphite powder in an aluminum holder. The expected signal was thus a combination of the diffuse non-spin flip, coherent scattering of the graphite powder plus a diffuse incoherent scattering from the hydrogen, with the usual 2/3 spin-flip scattering characteristic [18]. No difference in the spin-flip scattering is expected for the diffuse-incoherent only scattering with respect to field orientation, however the scattering experiment is performed in the 3 orthogonal directions in order to verify equivalence of the data and confirm that no artefacts come from the PASTIS or guide field installation. This sample was also measured after drying it in a 100°C oven for 2 hours, but for only one field direction. Polarized beam transmissions over time taken during these measurements are used to find the total beam polarization P_n at different times during the measurement, these data are shown in fig. 6.

While the beam intensity was sufficient for statistics on the transmitted beam, the scattered beam however, even after one hour of integration, provided only on the order of 10,000 counts for the entire spectrum from 1.6 \AA to 6.5 \AA . Even after binning the data in 0.25 \AA steps, the relative errors remain on the order of 5-10% for the raw data, and since the transmission

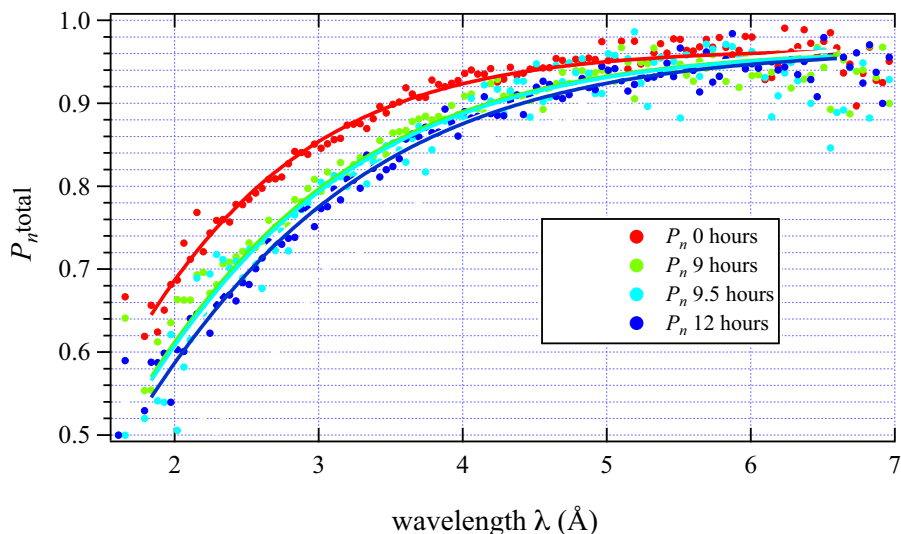


Figure 6. (total neutron polarization) Graph of the neutron polarization vs wavelength at different times and field orientations during our overnight measurement. The solid lines are fits of the data to $P_n = P_p \tanh(P_{He} \Theta \lambda)$.

of the empty cell used was anomalously low w.r.t. the sample measurements (a different but “identical” aluminum cell was used for the empty cell attempt) conclusions from the scattered-beam measurements are not readily obtainable. The data was however processed to separate the fraction of incoherent scattering from the coherent scattering as in [19, 20] and we did not see statistically significant differences in the scattered beam for the 3 different directions of the hydrated sample.

5. Conclusion and next steps

In realistic experimental conditions we have verified that the magic PASTIS field system and guide field configuration can perform to desired specifications in real world conditions. The ^3He lifetime met the desired benchmark of over 100 hours on beam while performing a number of X-Y-Z field directions changes that one might employ during a measurement. The neutron polarization transport was also verified to be adiabatic in agreement with the magnetic field calculations, up to the shortest available neutron wavelength of this instrument which was 1.6 Å. The control of the 11 power supplies used to control both the magic PASTIS system and the guide fields functioned as required to enable us to switch between field directions simply and quickly without losses of ^3He polarization.

Consequently further practical testing and proof-of-principle work is justified with actual TOF spectroscopy measurements, also with samples of scientific interests. In the near future we expect experiments to be conducted on NEAT at HZB [11] after the beam polarization is installed and commissioned and suitable long lifetime wide angle cells are available.

Acknowledgments

We acknowledge the many people who have contributed to the PASTIS and magic PASTIS throughout the years, notable colleagues who have been involved in discussions and prior work towards this method include A K Petoukov (ILL), J R Stewart (ISIS), K H Andersen (ESS), J Stride (Univ. of South Wales), T R Gentile, W C Chen and A Kirchhoff (NIST). We also

thank the technical support of the JCNS at MLZ in Garching and Jülich, the support of HZB, J. Plomp and A. Kusmin (TU Delft) who provided some equipment on V20 (fig. 2) and the students T. Theisselmann, J. Schmeissner, and D. Starostin who have assisted with the JCNS ^3He project over the years. Partial funding and support have come from the BMBF through the ESS design update project 05E10CJ1.

References

- [1] Voigt J, Soltner H, Babcock E, Aldus R J, Salhi Z, Gainov R R and Brückel T 2015 *EPJ Web of Conferences* **83** 03016 [DOI:10.1051/epjconf/20158303016]
- [2] Stewart J R, Andersen K H, Babcock E, Frost C D, Hiess A, Jullien D, Stride J A, Barthélémy J F, Marchal F, Murani A P, Mutka H, Schober H 2006 *Physica B* **385-386** 1142-1145 [DOI:10.1016/j.physb.2006.05.393]
- [3] Woracek R, Hofmann T, Bulat M, Sales M, Habicht K, Andersen K, Strobl M 2016 *Nuclear Instruments and Methods in Physics Research Section A* [DOI:10.1016/j.nima.2016.09.034]
- [4] Heil W, Andersen K H, Cywinski R, Humblot H, Ritter C, Roberts T W, and Stewart J R 2002 *Nuclear Instruments and Methods in Physics Research A* **485** 551-570 [DOI:10.1016/S0168-9002(01)00926-3]
- [5] Chen W C, Gentile T R, Ye Q, Kirchoff A, Watson S M, Rodriguez-Rivera J A, Qiu Y, Broholm C 2016 *J. of Physics Conference Series* **746(1)** 012016 [DOI:10.1088/1742-6596/746/1/012016]
- [6] Rols S, *ILL Endurance Brochure* 2013 **PANTHER** p. 26
http://wwwnew.ill.fr/fileadmin/users_files/documents/links/documentation/ILL_Endurance_Brochure_6Mo.pdf
- [7] Andersen K H, Jullien D, Petoukhov A K, Mouveau P, Bordenave F, Thomas F, Babcock E 2009 *Physica B* **404** 2652-2654 [DOI:10.1016/j.physb.2009.06.054]
- [8] Beecham C J, Boag S, Frost C D, McKetterick T J, Stewart J R, Andersen K H, Bentley P M, Jullien D 2011 *Physica B* **406** 2429-2432 [DOI:10.1016/j.physb.2010.11.054]
- [9] Winn B, Filges U, Garlea V O, Graves-Brook M, Hagen M, Jiang C, Kenzelmann M, Passell L, Shapiro S M, Tong X, 2015 *EPJ Web of Conferences* **83** 03017 [DOI:10.1051/epjconf/20158303017]
- [10] Carlile C J, et al., Technical Design Report for the European Spallation Source *European Spallation Source* 2013 [DOI:10.13140/RG.2.1.2040.6483/1]
- [11] Günther G, Russina M 2016 *Nuclear Instruments and Methods in Physics Research Section A* **828** 250-261 [DOI:10.1016/j.nima.2016.05.022]
- [12] Stewart J R, Deen P P, Andersen K H, Schober H, Barthélémy J-F, Hillier J M, Murani A P, Hayesband T, Lindenau B 2009 *J. of Applied Crystallography* **42** Issue 1 69-84 [DOI:10.1107/S0021889808039162]
- [13] Heinz Maier-Leibnitz Zentrum, DNS: Diffuse scattering neutron time-of-flight spectrometer 2015 *J. of large-scale research facilities* **1** A27 [DOI:10.17815/jlsrf-1-33]
- [14] Salhi Z, Babcock E, Gainov R, Bussmann K, Kämmerling H, Pistel P, Russina M, Ioffe A 2016 *J. of Physics Conference Series* **711(1)** 012013 [DOI:10.1088/1742-6596/711/1/012013]
- [15] Strobl M, Bulat M, Habicht K 2013 *Nuclear Instruments and Methods in Physics Research Section A* **705** 74-84 [DOI:10.1364/OE.23.000301]
- [16] Chupp T E, Coulter K P, Kandes M, Sharma M, Smith T B, Jones G, Chen W C, Gentile T R, Rich D R, Lauss B, Gericke M T, Gillis R C, Page S A, Bowman J D, Penttila S I, Wilburn W S, Dabaghyan M, Hersman F W, Mason M 2007 *Nuclear Instruments and Methods in Physics Research Section A: Accelerators, Spectrometers, Detectors and Associated Equipment* **574** 500-509. [DOI: 10.1016/j.nima.2007.02.091]
- [17] Salhi Z, Babcock E, Pistel P, Ioffe A 2014 2014 *J. of Physics Conference Series* **528(1)** 012015 [DOI:10.1088/1742-6596/528/1/012015]
- [18] Moon R M, Riste T, Koehler W C, 1969 *Phys. Rev.* **181** 920 [DOI:10.1103/PhysRev.181.920]
- [19] Gentile T R, Jonesa G L, Thompson A K, Barker J, Glinka C J, Hammouda B, Lynn J W 2000 *Journal of Applied Crystallography* **33(33)** 771-774 [DOI: 10.1107/S0021889800099817]
- [20] Babcock E, Salhi Z, Appavou M-S, Feoktystov A, Pipich V, Radulescu A, Ossovyi V, Staringer S, Ioffe A 2013 *Physics Procedia* **42** 154-162 [DOI: 10.1016/j.phpro.2013.03.190]